

Photoluminescence of Si Nanosolids near the Lower End of the Size Limit

L. K. Pan, C. Q. Sun,* B. K. Tay, T. P. Chen, and S. Li

*School of Electrical and Electronic Engineering, Nanyang Technological University, Singapore 6397987**Received: August 5, 2002*

Understanding the blue shift in the photoluminescence (PL) of the nanosolid near the lower end of the size limit ($D < 5$ nm) seems difficult with the currently available models. This challenges are not simply numerical convergency but importantly new physics hiding behind. We examined hereby the PL blue shift of Si nanosolids smaller than 3 nm both experimentally and theoretically, leading to a conclusion that a recent “bond order-length-strength” (bond-OLS) correlation mechanism is necessary. Agreement between predictions and observations reveals that the Si–Si surface bond contracts more significantly (by $\sim 20\%$) for the smallest Si nanosolid of which the PL blue shift corresponds directly to the rise of a single bond energy of the surface atom with much lowered coordination.

The discovery of efficient photoluminescence (PL) from porous silicon (PS) in 1990¹ has attracted tremendous effort on the tunable optical properties of semiconductive nanosolids. As a first-order approximation, the tunable PL property is often correlated to the size of the luminescent nanostructures. Simple particle-in-a-box calculation² adopts the trapping potential of an isolated atom to the nanosolid, leading to the analogue of “quantum box”. This convention determined that band-gap widening occurs when the dot size is reduced to the order of nanometers. However, quantitative correlation between the band gap and the dot dimension (D) has not yet produced convincing results for solid near the lower end of the size limit (< 5 nm). One often expects that the blue shift follows a $\Delta E_G(D)/E_G(\infty) \propto D^{-n}$ law ($n = 2,^2 1.16,^3 1.3,^4 1.37^5$). However, an effective mass approximation⁶ confirmed that the D^{-n} dependence suits only for crystallites larger than several nanometers. Not surprisingly, serious convergence problems arise when the solid is very small. This is not simply a numerical issue but is important conceptually, which forms the focus of our concern.

PS with Si particles smaller than 3 nm has been prepared in this work to examine the PL property at the lower end of the size limit in comparison with prediction based on the recent “bond order-length-strength” (bond-OLS) correlation mechanism.⁷ Porous Si samples were prepared using a (100)-oriented p-type Si wafer with a resistivity of 1–25 Ω cm in a $\text{HF}:\text{C}_2\text{H}_5\text{OH}:\text{H}_2\text{O}$ solution, where the weight ratios were 1:5:4. The (111)-oriented n-Si with a resistivity of 0.005–0.02 Ω cm was used as the cathode to obtain a more homogeneous electric field in the electrolyte, leading to samples with very uniform surfaces.⁸ After anodization, all the PS samples were dried by pentane. The dot size is controlled by varying the current density and characterized using an atomic force microscope (AFM). The band gap of the PS was measured under CW Xe lamp ($\lambda = 458$ nm) excitation with a SPEX FLUOROLOG-3 spectrofluorometer in an ambient environment. A typical AFM image and the PL spectra are shown in Figure 1, and information for dot sizes and the PL peaks for the PS samples is given in Table 1.

The porous silicon skeleton is often modeled as sponge, which consists of spherically shaped clusters with all the Si atoms

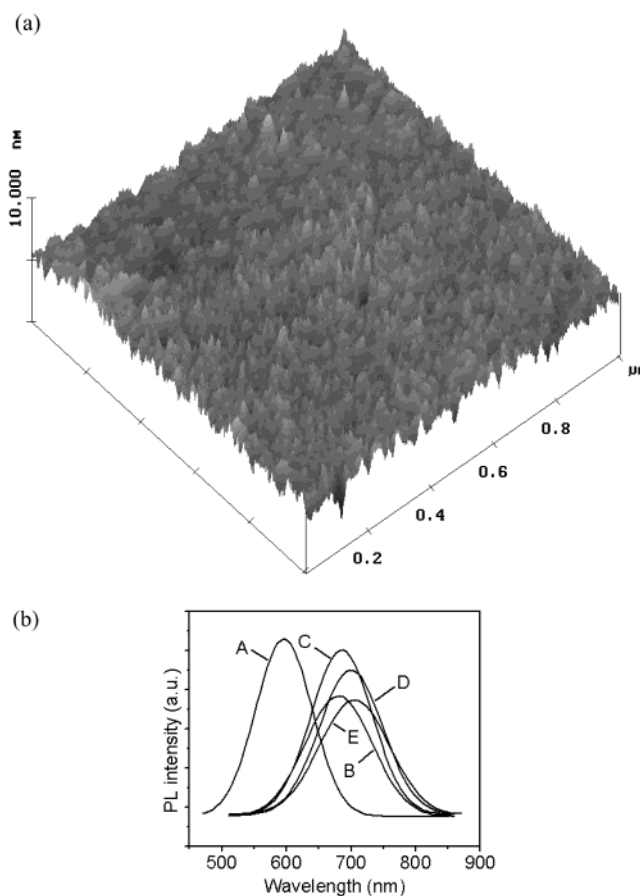


Figure 1. (a) Typical AFM image of as-anodized PS formed on p-type Si ($D \sim 3$ nm, $R_{\text{rms}} = 1.44$ nm) and (b) PL spectra showing the blue shift.

located at the sites of a diamond lattice. All the dangling bonds of atoms in the outer shells of the cluster are saturated with hydrogen atoms.⁹ For the Si cluster of $D \leq 1$ nm, the nearest CN of the first shell reduces to $1/3 \sim 1/4$ of the bulk value¹⁰ due to the higher surface curvature. On the other hand, the portion of surface atoms relative to the total number of atoms in the particle increases to unity. It is understandable that when a

* Corresponding authro. E-mail: ecqsun@ntu.edu.sg. Fax: 65 6792 0415. <http://www.ntu.edu.sg/home/ecqsun/>.

TABLE 1: Summary of the Experimental Conditions and the Measured Size and PL Energies of PS at the Lower End of the Size Limit

sample	current density (mA/cm ²)	PL peak (nm)	E_G (eV)	D (nm)
A	80	595.82	2.08	1.4 ± 0.2
B	60	680.76	1.82	1.7 ± 0.2
C	50	685.57	1.81	2.0 ± 0.2
D	40	692.17	1.79	2.4 ± 0.2
E	30	705.15	1.76	2.8 ± 0.3

D stands for the mean diameter of the Si nanocrystals which form the p-Si skeleton.

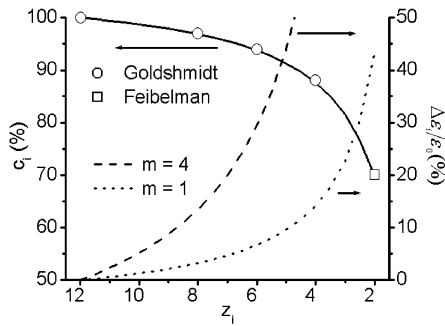


Figure 2. Illustration of the bond-OLS correlation mechanism which states that the CN imperfection of an atom causes the remaining bonds of this lower-coordinated atom to contract ($d_i = c_i d$) spontaneously associated with bond energy rise ($\epsilon_i = c_i^{-m} \epsilon$; $m = 1$ for elemental solid and $m = 4$ for compounds or alloys). Data of open circles and open squares are sourced from Goldschmidt¹¹ and Feibelman.¹²

particle reduces its size from nanometric to atomic scale, the nanosolid degenerates to an isolated atom with discrete energy levels. Therefore, the band gap expansion can never be larger than the separation of the corresponding energy levels.

The bond-OLS premise⁷ indicates that (i) the atomic radius of a surface atom relaxes spontaneously because of the reduced atomic CN at the surface, (ii) the bond energy of the relaxed bond increases because of the spontaneous relaxation, (iii) the bond energy rise increases the energy density in the relaxed region because the number of bonds does not change between any two neighboring circumferential atomic layers with relaxation, and (iv) the density rise of binding energy in the relaxed region contributes to the Hamiltonian of the solid that determines the entire band structure of a nanosolid including the band gap, core-level shift, bandwidth, and the band tails through modifying the crystal field. As illustrated in Figure 2, the bond-OLS correlation can be formulated as

$$\begin{cases} d_i = c_i d \\ \epsilon_i(d_i) = c_i^{-m} \epsilon(d) \\ c_i(z_i) = 2 / \{1 + \exp[(12 - z_i)/(8z_i)]\} \end{cases} \quad (1)$$

where d_i and d are the bond length of atoms in the i th atomic layer and of atoms in the bulk. $\epsilon_i(d_i)$ and $\epsilon(d)$ are the corresponding bond energies at equilibrium atomic separation. z_i is the effective CN of an atom in the i th atomic layer. Normally, for the outermost two atomic layers of a flat plate $z_1 = 4$ and $z_2 = 6$. At the lower end of size limit of a spherical dot, $z_1 \leq 3$. c_i^{-m} describes the energy change with the reduced bond length. m , being an adjustable parameter, varies with the nature of the bond. Progress^{7,15,19,20} so far reveals that for elemental solid, $m = 1$; for compounds and alloys, $m = 4$. $c_i(z_i)$ is formulated on the basis of Goldschmidt's premise¹¹ and Feibelman's finding¹² on the dimer bond contraction of Ti, Zr,

Mo, and V. According to Goldschmidt, if the CN reduces from 12 to 8, 6, and 4, the corresponding ionic radius will shrink by 3%, 4%, and 12%. Except for some II-a (Be, Mg(0001) surface) and II-b (Zn, Cd, Hg dimer bond) elements that are reported to expand, all the elemental dimer bonds contract by even as high as 30%–40% for Ti, Zr, V, and Mo, for example. It should be emphasized that the bond-OLS premise involves no assumptions or freely adjustable parameters or even the particular form of the interatomic potential.

There is profound evidence for the bond-OLS mechanism. For instance, the first interlayer spacing of diamond (111) has been reported to contract by 30%.¹³ A contraction by 4%–12% of the O–Cu bond has been found to form one of the four essential stages in the O–Cu (001) surface bonding kinetics.¹⁴ A 12%–14% contraction of the N–Ti/Cr bond has been confirmed to enhance the surface stress by up to 100%.¹⁵ Most strikingly, a recent density functional theory calculation¹⁶ reveals that for Au, Cu, Pt, Pd, Ni, and Ag single atomic chains, the binding energy per bond is (–3 to –1 eV), 2 to ~3 times larger in the chains than the single bond energy (–1 τ o ~–0.4 eV) of the bulk fcc structures and the equilibrium atomic separation contracts by 10% (for Cu and Ag) ~15% (for Pt). These findings concur with the bond-OLS premise though the extent of relaxation and energy rise differ slightly. Efforts made so far have shown consistently that the bond contraction at a surface dominates the size-and-shape dependency of nanometric materials in many aspects such as the mean lattice contraction,¹⁷ blue shift in photoluminescence,^{18,19} dielectric suppression,²⁰ critical temperature for ferromagnetic phase transition,²¹ and melting point change²² of nanomaterials as well as the transition behavior of ferro- and pyroelectrics of PbZrTi oxides.^{23,24}

Considering the contribution from the outermost relaxed atomic layers, the Hamiltonian of a nanosolid is given as^{7,25}

$$\begin{aligned} \hat{H}(D) &= \hat{H}_{\text{atom}}(r) + \hat{H}_{\text{crystal}}(D) \\ \hat{H}_{\text{atom}}(r) &= -\frac{\hbar^2 \nabla^2}{2\mu} + v_{\text{atom}}(r) \\ \hat{H}_{\text{crystal}}(D) &= V_{\text{crystal}}(\infty)[1 + \delta_{\text{surf}}] \end{aligned} \quad (2)$$

$v_{\text{atom}}(r)$ is the potential of intra-atomic trapping of an isolated atom and $V_{\text{crystal}}(\infty)$ is the crystal field of an extended solid that sums the interatomic binding potential over the solid. According to the band theory,²⁶ the gap between the conduction and the valence band of an extended solid expands from $E_G(\infty)$ to $E_G(D)$:

$$E_G(D) = E_G(\infty)[1 + \delta_{\text{surf}}] \quad (3)$$

δ_{surf} represents the effect of surface relaxation:

$$\delta_{\text{surf}} = \sum_{i \leq 3} \gamma_i \frac{\Delta v(d_i)}{v(d)} = \begin{cases} c_i^{-m} - 1 & D \sim 1 \text{ nm} \\ \sum_{i \leq 3} \gamma_i (c_i^{-m} - 1) & D \gg 1 \text{ nm} \end{cases} \quad (4)$$

where $v(d_i)$ is the binding energy density in the relaxed region, and $v(d_i) \propto \epsilon_i(d_i)$. γ_i is the portion of atoms in the i th atomic layer compared to the total number of atoms of the entire solid of different dimensionality ($\tau = 1$ –3 corresponds to a plate, a rod and a spherical dot, respectively), which is given as

$$\gamma_i = \frac{N_i}{N} = \frac{V_i}{V} = \frac{\tau}{K} \left(1 - \frac{i - 0.5}{K}\right)^{\tau-1} c_i \quad (D = 2Kd) \quad (5)$$

It is interesting to note (eq 4) that at the lower end of the size limit, the $\Delta E_G(D)/E_G(\infty) = \delta_{\text{surf}}$ corresponds directly to the

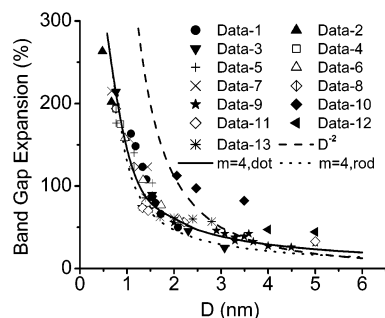


Figure 3. Comparison of the predictions with observations on the D dependence of the PL of PS. Theoretical results: Data-1,⁹ Data-2,²⁷ Data-3,²⁸ Data-4,²⁹ Data-5,³⁰ Data-6,³¹ Data-7,³² Data-8,³³ Measurements: Data-9,³⁴ Data-10,⁶ Data-11,¹⁰ Data-12,³⁵ and Data-13 (current results).

TABLE 2: Parameters for the Band-Gap Expansion of Porous Silicon

	E_G (bulk) (eV)	d (nm)	z_1	z_2 ($K > 2$)	m
porous silicon	1.12	0.263	3,4	6	4

relative increase of a single bond energy as $\gamma_1 \sim 1$, $\gamma_2 = \gamma_3 = 0$, and it is independent of the dimensionality (Figure 3).

The size-dependent PL shift of the Si nanosolid obtained herewith and by others is compared with predictions using parameters given in Table 2. Figure 3 shows the matching between observations and predictions for spherical dot and rod like structures. Apparently, simulation based on the D^{-2} convention diverges from observations near the lower end of size limit. As expected, prediction based on the bond-OLS premise not only converges theory to observations but also provides interpretation that goes beyond existing D^{-n} conventions.

Most strikingly, the bond-OLS involves no assumptions or freely adjustable parameters. What we have used is the fact of CN-imperfection-induced bond energy rise, which links the PL blue shift of the smallest nanosolid directly to the rise of single bond energy of a surface atom with much lowered CN.

References and Notes

- (1) Canham, L. T. *Appl. Phys. Lett.* **1990**, *57*, 1046.
- (2) Kalkhoran, N.; Namavar, F.; Maruska, H. P. *Appl. Phys. Lett.* **1993**, *63*, 2661.

- (3) Fu, H.; Zunger, A. *Phys. Rev. B* **1997**, *55*, 1642.
- (4) Albe, V.; Jouanin, C.; Bertho, D. *Phys. Rev. B* **1998**, *58*, 4713.
- (5) Micic, O. I.; Sprague, J.; Lu, Z.; Nozik, A. J. *Appl. Phys. Lett.* **1996**, *68*, 3150.
- (6) Kanemitsu, Y.; Uto, H.; Masumoto, Y.; Matsumoto, T.; Futagi, T.; Mimura, H. *Phys. Rev. B* **1993**, *48*, 2827.
- (7) Sun, C. Q.; Chen, T. P.; Tay, B. K.; Li, S.; Huang, H.; Zhang, Y. B.; Pan, L. K.; Lau, S. P.; Sun, X. W. *J. Phys. D* **2001**, *34*, 3470.
- (8) Andersen, O. K.; Veje, E. *Phys. Rev. B* **1996**, *53*, 15643.
- (9) Wang, X.; Huang, D. M.; Ye, L.; Yang, M.; Hao, P. H.; Fu, H. X.; Hou, X. Y.; Xie, X. D. *Phys. Rev. Lett.* **1993**, *71*, 1265.
- (10) Schuppler, S.; Friedman, S. L.; Marcus, M. A.; Adler, D. L.; Xie, Y. H.; Ross, F. M.; Chabal, Y. J.; Harris, T. D.; Brus, L. E.; Brown, W. L.; Chaban, E. E.; Szajowski, P. F.; Christman, S. B.; Citrin, P. H. *Phys. Rev. B* **1995**, *52*, 4910.
- (11) Goldschmidt, V. M. *Ber. Deutsch. Chem. Ges.* **1927**, *60*, 1270.
- (12) Feibelman, P. J. *Phys. Rev. B* **1996**, *53*, 13740.
- (13) Halicioglu, T. *Surf. Sci.* **1991**, *259*, L714.
- (14) Sun, C. Q. *Vacuum* **1997**, *48*, 535.
- (15) Sun, C. Q.; Tay, B. K.; Lau, S. P.; Sun, X. W.; Zeng, X. T.; Bai, H.; Liu, H.; Liu, Z. H.; Jiang, E. Y. *J. Appl. Phys.* **2001**, *90*, 2615.
- (16) Bahn, S. R.; Jacobsen, K. W. *Phys. Rev. Lett.* **2001**, *87*, 266202.
- (17) Sun, C. Q. *J. Phys. Condens. Matter* **1999**, *11*, 4801.
- (18) Sun, C. Q.; Gong, H. Q.; Hing, P.; Ye, H. T. *Surf. Rev. Lett.* **1999**, *6*, L171.
- (19) Sun, C. Q.; Sun, X. W.; Gong, H. Q.; Huang, H.; Ye, H.; Jin, D.; Hing, P. J. *Phys. Condens. Matter* **1999**, *11*, L547.
- (20) Sun, C. Q.; Sun, X. W.; Tay, B. K.; Lau, S. P.; Huang, H.; Li, S. *J. Phys. D* **2001**, *34*, 2359.
- (21) Zhong, W. H.; Sun, C. Q.; Tay, B. K.; Li, S.; Bai, H. L.; Jiang, E. Y. *J. Phys. Condens. Matter* **2002**, *14*, L399.
- (22) Sun, C. Q.; Wang, Y.; Tay, B. K.; Li, S.; Huang, H.; Zhang, Y. J. *Phys. Chem. B* **2002**, *106*, 10701.
- (23) Huang, H.; Sun, C. Q.; Hing, P. J. *Phys. Condens. Matter* **2000**, *12*, L127.
- (24) Huang, H.; Sun, C. Q.; Zhang, T. S.; Hing, P. *Phys. Rev. B* **2001**, *63*, 184112.
- (25) Sun, C. Q.; Tay, B. K.; Zeng, X. T.; Li, S.; Chen, T. P.; Zhou, J.; Bai, H. L.; Jiang, E. Y. J. Bond order-length-strength (Bond-OLS) correlation mechanism for the shape and size dependency of a nanosolid. *Phys. Condens. Matter*, **2002**, *14*, 7781.
- (26) Omar, M. A. *Elementary Solid State Physics: Principles and Applications*; Addison-Wesley: New York, 1975.
- (27) Dorigoni, L.; Bisi, O.; Bernardini, F.; Ossicini, S. *Phys. Rev. B* **1996**, *53*, 4557.
- (28) Sanders, G. D.; Chang, Y. C. *Phys. Rev. B* **1992**, *45*, 9202.
- (29) Hybertsen, M. S.; Needels, M. *Phys. Rev. B* **1993**, *48*, 4608.
- (30) Ohno, T.; Shiraishi, K.; Ogawa, T. *Phys. Rev. Lett.* **1992**, *69*, 2400.
- (31) Yeh, C. Y.; Zhang, S. B.; Zunger, A. *Phys. Rev. B* **1994**, *50*, 14405.
- (32) Read, A. J.; Needs, R. J.; Nash, K. J.; Canham, L. T.; Calcott, P. D. J.; Qteish, A. *Phys. Rev. Lett.* **1992**, *69*, 1232.
- (33) Polatoglou, H. M. *J. Lumin.* **1993**, *57*, 117.
- (34) Canham, L. *Properties of Porous Silicon*; INSPEC: London, 1997; p 213.
- (35) Pavesi, L.; Giebel, G.; Ziglio, F.; Mariotto, G.; Priolo, F.; Campisano, S. U.; Spinella, C. *Appl. Phys. Lett.* **1994**, *65*, 2182.